

# TURBULENCE SUPPRESSION IN A SUPERSONIC JET WITH WATER INJECTION

A. Krothapalli, L. Venkatakrishnan, R. Elavarasan and L. Lourenco  
Fluid Mechanics Research Laboratory  
Department of Mechanical Engineering  
2525 Pottsdamer Street  
Florida A&M University and Florida State University  
Tallahassee, FL 32310  
[kroth@fmrl.fsu.edu](mailto:kroth@fmrl.fsu.edu)

## ABSTRACT

*An experimental investigation has been carried out on a supersonic jet of air issuing from an  $M = 1.44$  converging-diverging rectangular nozzle of aspect ratio 4. The jet structure was obtained using Particle Image Velocimetry. The effect of small amount of water (~5% of the mass flow rate of the jet) injected into the shear layers of the jet, on the unsteady flow structure were examined. The presence of the water droplets in the jet modified the turbulence structure significantly resulting in the rms velocities reduction greater than 30% as compared to that of a normal jet. Similar reductions of the forcing term of the Phillip's equation (1960), that represents the generation of the pressure fluctuations in the jet, were also found.*

## 1. INTRODUCTION

In need of a rational approach to the supersonic jet noise suppression, fundamental studies are being conducted in our laboratory using modern experimental techniques. Recognizing that an essential prerequisite is that the nature and location of the important noise sources be clearly understood, our work is first focused on describing the unsteady flow of the supersonic jet in some detail using Particle Image Velocimetry (PIV). In this paper we describe the flow and acoustic characteristics of an  $M = 1.44$  ideally expanded rectangular jet. In addition, we explore the effect of a moderate amount of water injection on the flow and noise characteristics of the supersonic jet.

This paper presents a novel approach for the suppression of the dominant mixing noise sources in a supersonic jet. Water droplets are injected into the jet to manipulate the dominant source region. The dispersed droplets serves to attenuate the turbulent kinetic energies of the gas phase in the noise-producing region of the jet. The strength of the attenuation is expected to depend up on the mass of water injected (mass

loading), the droplet size and the injection location.

Sound attenuation due to the presence of water droplets in air has been a subject of research since 1948 (Knudsen et al, 1948). Marble et al (1970, 1975) conducted theoretical investigation to determine the sound attenuation in ducts by vaporization of liquid droplets.

In the present investigation we limit the amount of water injected to a small fraction of the total mass of the jet ( $m_{H_2O}/m_{air} < 0.1$ ). Our focus in the present investigation is to determine the effect of water droplets on the unsteady flow field of a supersonic jet operating at the ambient temperature. The evaporation effects of droplets are considered in a separate investigation that is being carried out presently.

## 2. APPARATUS, INSTRUMENTATION AND PROCEDURES

The experiments were conducted in the blow-down compressed air facility of the Fluid Mechanics Research laboratory at the Florida State University. A high-displacement reciprocating air compressor drives the facility, which is capable of supplying air at a maximum storage pressure of 160 bars. The air can be heated by passing through an array of resistive tank heaters having a maximum power output of 450 kW and capable of achieving stagnation temperatures up to 700 K. The  $M = 1.44$  jet used in this study can be run continuously for about 40 Mts.

The blowdown facility was fitted with a rectangular nozzle having an exit aspect ratio of 4:1. The dimensions of the nozzle in the exit plane measured, height,  $h = 10$  mm by width,  $W = 40$  mm. The contour of the short dimension of the nozzle was generated using the method of characteristics for a design Mach number of 1.44. The walls of the long dimension of the nozzle were parallel downstream of the throat. The circular dimension of the connecting pipe upstream of the throat was blended to facilitate a

smooth transition to a rectangular cross section. During all experiments the ratio of the stagnation to ambient pressures was held nominally 3.37 as required for isentropically expanded flow at Mach 1.44. The jet was operated at a stagnation temperature of 335 K to avoid problems of condensation associated with the humid Florida air.

The mean exit velocity profile with laminar boundary layers was tophat. The jet was exhausted into a quiet surrounding at ambient conditions. The centerline mean exit velocity,  $U_1$ , is measured to be about 420 m/sec, corresponding to a Reynolds number based on the nozzle height of about  $2.8 \times 10^5$ . The convective Mach number of the initial shear layer  $M_c = (U_1 - U_2) / (a_1 + a_2)$ , where the subscripts 1 and 2 denote the primary and secondary streams, respectively and  $a$  represents the speed of sound, is about 0.64.

The jet was seeded with small ( $\sim 1 \mu m$ ) oil droplets generated using a modified Wright nebulizer. The ambient air was seeded with smoke particles ( $1\text{--}5 \mu m$  in diameter) produced by a Rosco fog generator. Larger particles are entrained into jet and are confined mostly to sub-sonic region. Recent measurements obtained in an underexpanded jet created using the same apparatus showed that the velocity measurements obtained using PIV are in close agreement with those derived from total and static pressure measurements (Alkislar; 2000). In spite of the fact that the particles were exposed to relatively weak compression and expansion of the flow within the shock cells, very little particle lag was noticed in the measurements. In the present experiment, the nozzle being operated at the ideally expanded condition, no shock cells were observed. The velocity of the particles was found to be in close agreement ( $\pm 1\%$ ) with the calculated exit velocity using isentropic relations.

### 2.1 Particle Image Velocimetry

Non-intrusive measurements of the velocity field were made using Particle Image Velocimetry (PIV). When necessary, a stereoscopic PIV was also used. A detailed discussion of the application of the Stereoscopic PIV technique to supersonic jets is given in Alkislar et al (2000).

The CCD camera used to capture the images had a resolution of 1008(H)  $\times$  1018(V) pixels with the size of  $9 \times 9 \mu m$ , and a maximum frame rate of 30 Hz. The camera was equipped with a 58.37 mm focal length lens that was specifically designed for the wavelength of the laser light. To illuminate the flow-field, a frequency doubled Nd-Yag laser with dual cavity (Spectra-

Physics PIV-400) was used. The time  $\Delta t$  between the two laser pulses was kept at  $1.3 \mu sec$ . The camera was positioned at  $90^\circ$  angle to the jet axis. The optical arrangement was set such that the image area covered was about 12cm  $\times$  12cm.

### 2.2. Water Injection

The configuration employed to establish water injection into the shear layer is shown in figure 1. The water was atomized and injected into the jet by means of four 1993 Mitsubishi Eclipse fuel injectors (Model MPFI 629-098 Type 1.8L) – two for each shear layer. The injectors were pressurized to 1.55 MPa, and pulsed at 100 Hz. The injectors were located at 13 heights

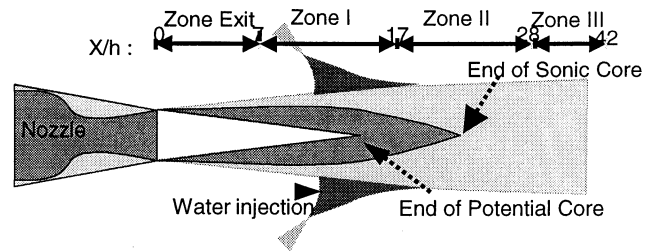


Figure 1. Schematic of the jet with water injection.

above and below the jet centerline and at an angle of  $16^\circ$  to it. The water exited the injectors as a spray cone. Expecting that the noise-producing region being located at several heights down stream of the nozzle exit, most of the detailed investigations were carried out with the water injected into the shear layer covering the region from 10h to 17h (zone I in figure 1). The mass of the water injected was limited to 5% of the jet mass flow. The resulting volume flow rate is about 1.0 L / minute.

### 2.2a Water Droplet Characteristics

A brief study was performed to obtain the relevant characteristics of drops and their evolution by the measurement of bubble-size probability density functions using a TSI Phase Doppler Particle Analyzer (PDPA/LDV) system Rev. 2.0 RSA. These measurements were used primarily to determine the droplet diameter at different locations in the jet. This study is not intended to provide a detailed account of the breakup mechanisms of liquid drops injected into a transverse high velocity air stream. The reader is referred to recent papers (Chou et al, 1997 and Liu and Reitz, 1997) and the references there in, on this subject. However, the resulting droplet characteristics are important here to assure that the

PIV velocity measurements accurately represent the flow physics described later.

The PDPA instrument used in this study was capable of measuring drop diameters from 0.5  $\mu\text{m}$  to 170  $\mu\text{m}$ . The primary jet was not seeded during PDPA measurements. The Arithmetic mean diameter ( $D^{10}$ ) was found to be 140  $\mu\text{m}$  (Krothapalli et al, 2000). The velocity of the drops at the injector exit was 20m/s and decreases to about 10m/s at the edge of the shear layer. From the PIV measurements, the magnitude of the free jet entrainment velocity was also found to be about 10 m/sec, suggesting that the drops enter the shear layer at the same velocity as the entrainment velocity.

The relative velocity between the drop and the gas varies from almost zero at the edge of the shear layer to about 400 m/s on the jet axis. In the region of interest, most of the droplets are found in the high-speed portion of the shear layer. Hence, for the purposes of calculating non-dimensional quantities, the relative velocity of the droplet is taken as 250 m/s. From this and other information, we can then calculate the non-dimensional quantities of interest as follows.

Weber Number of the drop:

$$We = \frac{\rho_G d_o u_o^2}{\sigma} = 142,$$

where  $d_o$ ,  $\sigma$  and  $u_o$  are the initial drop diameter, surface tension of the water and it's relative velocity to the flow respectively.  $\rho_G$  is the density of air. The subscripts L and G denote liquid and gas properties.

Reynolds number of the drop:

$$Re = \frac{\rho_G u_o d_o}{\mu_G} = 2250$$

Ohnesorge number:

$$Oh = \frac{\mu_L}{\sqrt{\rho_o d_o \sigma}} = 9.5 \times 10^{-3}$$

From the breakup regime map of Hsiang and Faeth (1995) when based on the Weber and Ohnesorge numbers calculated above, it is seen that the breakup process of the drops in the present study is of the shear type ( $10^2 < We < 10^3$ ,  $10^{-4} < Oh < 10^{-1}$ ).

Typical droplet size pdf measured at  $X/h = 26$  and  $Y/h = 1.5$  indicate that very few droplets having sizes greater than about 5  $\mu\text{m}$  exist in

the shear layer. As expected, the drops breakup quickly from an initial size of 140  $\mu\text{m}$  at the injector exits to a size of few microns. With increasing downstream distance, mean droplet diameter remains constant suggesting that the drop breakup process is mostly complete within the injection region and no more breakup takes place in the region where the PIV measurements are made. To ensure that no larger droplets were present in the region of the measurement, droplet size pdfs were obtained across the jet at several downstream locations. The data clearly show that the droplet size remain uniform across the jet. These observations are consistent with those of Martinez-Bazan et al. (1999).

Samimy and Lele (1991) have shown that the particle response is well characterized by a parameter  $\tau$ , the ratio of particle response time to the flow time scale, defined as

$$\tau = \frac{\tau_p}{\tau_f}$$

where

$$\tau_f = \frac{10\delta_{uo}}{(U_1 - U_2)}$$

$\delta_{uo}$  is the initial vorticity thickness

$$\tau_p = \frac{\rho_p d_p^2}{18\mu}$$

For the conditions of the present experiment, the parameter  $\tau$ , was estimated to be about 0.2. The arithmetic mean droplet diameter of 4  $\mu\text{m}$  was used in this estimation. Samimy and Lele (1991) show that the velocity measurement errors grow linearly with  $\tau$  with approximately 2% error for  $\tau = 0.2$ . Based on the above observations, and since both seeding particle and water droplet sizes are within the acceptable range, the PIV velocity measurements are expected to be within an uncertainty associated with an experiment of this nature, typically about 1 ~ 2%.

### 3. RESULTS AND DISCUSSION

Typical double exposure images of the jet with water injection are shown in figure 2. The main jet is seeded with oil droplets while the ambient medium is seeded with smoke particles. Due to the limitations of the CCD sensor resolution, the images were taken covering each region, as marked in figure 1, separately. For most of the results discussed here, the water is injected

in the region denoted in the figure as zone I. Because of the intense scattering of water droplets, they can be easily distinguishable from the seed particles in the PIV images as shown in figure 2. In zone I, shown in figure 2, most of the injected water is confined to the shear layer, indicating that the breakup of the large water drops takes

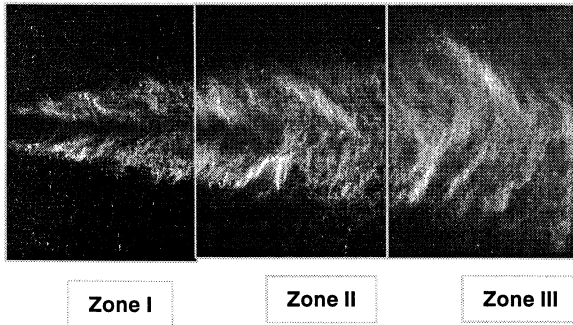


Figure 2. PIV images of the jet with water injection.

place in the shear layer. The measured droplet pdf at the end of this region and beyond, suggest that the breakup process was completed within the zone I, and the arithmetic mean droplet diameter at the end of the region was found to be 4  $\mu\text{m}$ . Velocity measurements in this zone were not obtained due to the difficulties encountered by the CCD sensor saturation and laser beam attenuation. Both of these are a result of dense cloud of relatively large diameter droplets and their intense scattering. In the region denoted as zone II and zone III, it is clearly seen that the water droplets migrate to the center of the jet. In addition, the water droplets populate the entire jet.

The instantaneous velocity field in zones II and III were obtained by the method described in section 2.1 with interrogation regions of 16x16 pixels corresponding to a physical dimension of 2.3mm x 2.3mm. The data was obtained using a 110 x 80 (X,Y) Cartesian grid. Typical instantaneous velocity fields in zone II corresponding to the normal jet and the jet with water injection (in zone I) are shown in figure 3. The velocity field is shown as uniformly scaled vectors. One thousand such instantaneous velocity fields were obtained for each of the conditions tested. It is to be noted that the velocity field described here is that of the gas phase (air jet) and most of the water droplets, being of the order of 1  $\mu\text{m}$  act like the seeding particles.

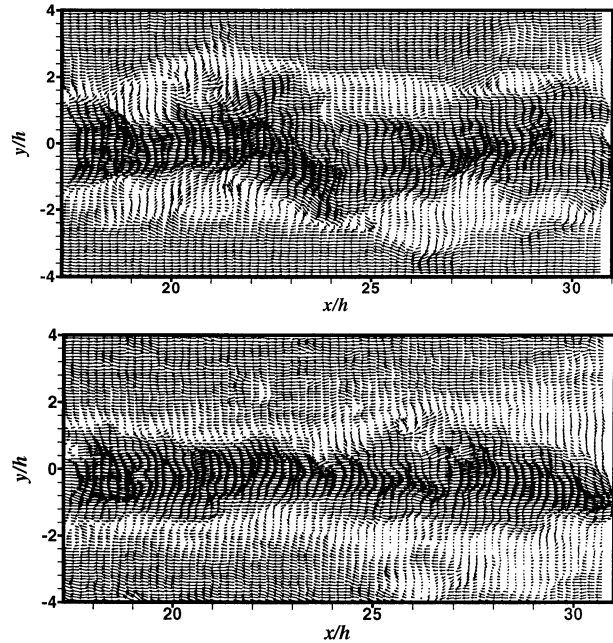


Figure 3. Instantaneous velocity fields in the post injection region. Top: normal jet; Bottom: with water injection.

To accentuate the large-scale vortical structures, the velocity field is plotted in a reference frame moving at a uniform velocity of 100 m/sec. When plotted in this fashion, large scale flapping motion of the natural jet is clearly depicted in figure 3a. The dominant effect of water injection is the reduction of the flapping motion of the jet. In addition, the size of the recognizable large-scale vortical structures is also reduced. A typical vortical structure in each picture is identified as shown in the figure. From a number of instantaneous pictures in zone II, the convection velocity of the large vortical structures was found to be about 50% of the local centerline velocity.

### 3.1 Mean flow structure

The mean velocity distribution covering the region from the nozzle exit to about 42h was obtained. The end of the potential core and the sonic core are found to be at 8h and 22h respectively. Except in the immediate neighborhood of the post injection region, the velocity fields in the jets with and without water injection are found similar, suggesting that the water injection has negligible effect on the mean flow structure. Figure 4 shows the distribution of the mean velocity  $U$  across the jet in the XY plane at selected downstream stations, ranging from 20 to 40 heights. The velocity  $U$  is normalized with re-

spect to the  $U_c$ , the centerline velocity at each station, while the distance  $Y$  is normalized by the corresponding half width  $b_{0.5}$ . The profiles are geometrically similar, within the limits of error for the experiment, for  $X$  greater than about 20h. This similarity persists even in the case of the jet with water injection

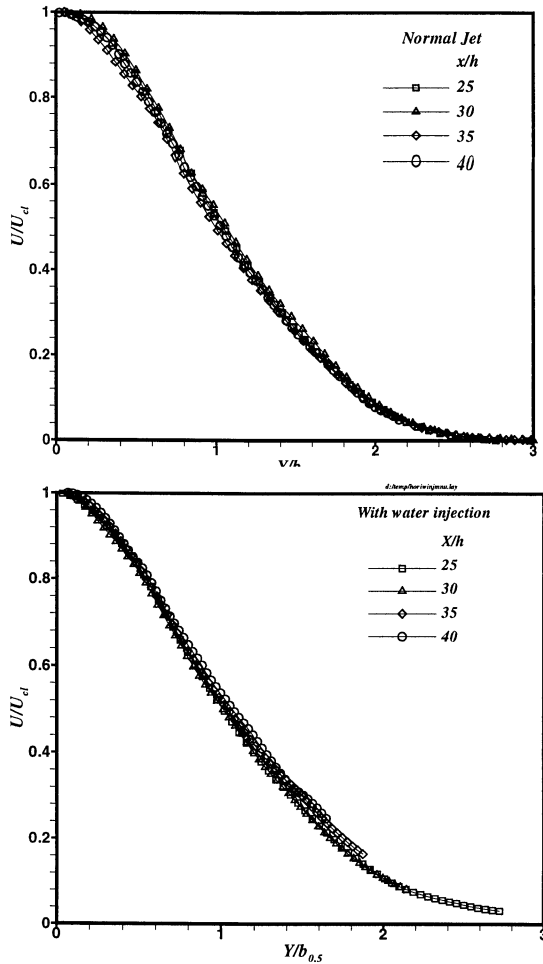


Figure 4. Normalized streamwise velocity profiles in the post injection region. Top: normal jet, Bottom: with water injection.

### 3.2 Turbulence characteristics

The magnitudes of the turbulence intensities increase sharply close to the jet exit reaching a peak at about 16h and subsequently remain unchanged with downstream distance. The peak values of axial and transverse turbulence intensities are observed to be about 0.125 and 0.085 respectively. The measured magnitudes are close to those of Lau et al., (1979), made in a  $M = 1.37$  axisymmetric jet. The location at which these peak amplitudes are observed is also consistent with their measurements. The excellent agreement of the present data with

those of Lau et al. (1979) suggests that the limited number of samples used in determining the rms intensities is sufficient. In the case of the jet with water injection, a significant reduction in transverse turbulence intensity is observed in the post injection region. As will be shown in figure 5 the reductions observed extend into the entire post injection region of the jet. The magnitude of the turbulence quantity shown in gray scale contours is superimposed on the mean velocity field in figure 5.

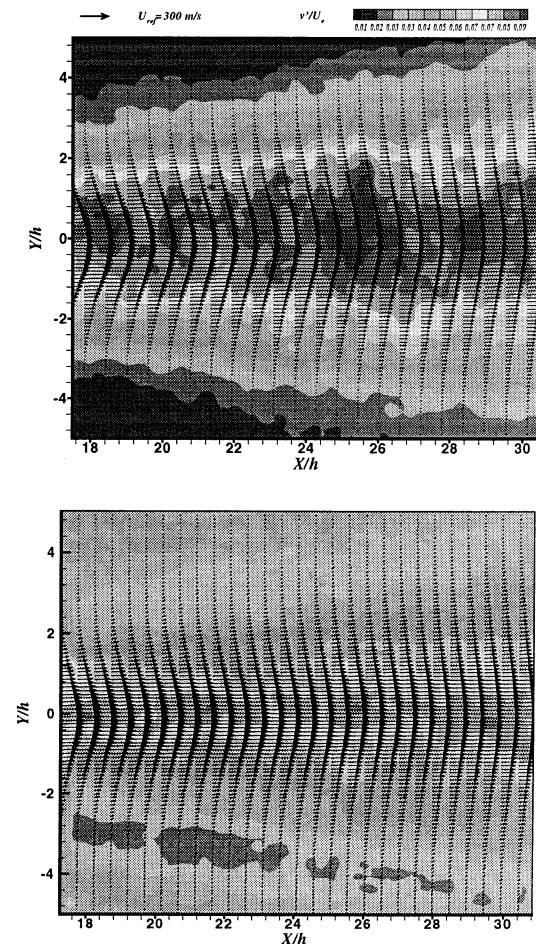


Figure 5. RMS distribution of the transverse component of the velocity in the post injection region. Top: normal jet, Bottom: with water injection.

The magnitudes of the turbulence intensities and the shear stress of the water-injected jet are substantially reduced as compared to those of the normal jet. The maximum reductions are found in the distribution of the transverse turbulence intensity and the shear stress. For example, the maximum intensity of  $v'$  fluctuations is about 0.08 and the contour corresponding to this level

covers almost the entire jet column. While in the case of the water-injected jet, the maximum contour level was decreased to about 0.055, almost a 30% reduction in magnitude. A much greater reductions (about 60%) are seen in the turbulent shear stress distribution. The reductions in the streamwise fluctuations are not as significant. Similar reductions are also seen in zone III, except the magnitude of the reductions seen are much lower. These measurements clearly indicate that the effect of water injection is to lower the turbulence intensities, (especially in  $v_{rms}$ ) and shear stress in the jet. Turbulence attenuation in particle laden flows although has been observed in shear flows (Kulick et al., (1994), most often the mass loading is much higher as compared to the present situation.

#### 4. CONCLUSIONS

A series of experiments were performed in an  $M = 1.44$  rectangular jet to examine the influence of water injection on the flow and noise characteristics. A water spray consisting of 140  $\mu\text{m}$  drops was injected into the shear layer of the jet, covering a region of about 7 heights, at two different locations, at the nozzle exit and at the end of the potential core. The mass flow rate of the water was substantially lower ( $\sim 5\%$  of the jet mass flow rate) than those found in earlier two-phase flow studies. Phase Doppler Particle analyzer measurements indicate that drops breakup quickly in the high-speed shear layer. At the end of the injection region, the drops are reduced to droplet clouds consisting of mostly 4 $\mu\text{m}$  or less size droplets.

Particle Image Velocity measurements in the post injection region indicate that the breakup process extending over an appreciable region results in significant turbulence attenuation.

Mean velocity field in the post injection region of the jet was found to be nearly identical with the normal jet to within the experimental uncertainty, suggesting that there was no apparent modification to the mean flow.

Using the instantaneous velocity field, obtained by PIV, and guided by the analysis of Phillips (1960), the source terms given by the velocity fluctuation gradients were estimated. From the magnitude variation of the terms with downstream distance, it is found that the noise-producing region in a supersonic jet extends from the nozzle exit to about 20 heights or the end of the supersonic core. The effect of water injection was to reduce the magnitude of the source terms. As suggested by the solution of the

Phillips equation, the measured sound field and source terms are reduced by the same amount.

#### 5. ACKNOWLEDGEMENTS

The work described in this paper was partly supported by the NASA Langley Research Center. We gratefully acknowledge the help of Dr. Debopam Das, Mr. Bahadir Alkislar and Mr. Vikram Siddavaram in acquiring some of the data.

#### 6. REFERENCES

1. Alkislar, M. B., Lourenco, L. M. and Krothapalli, A., 2000, "Stereoscopic PIV Measurements of a Screeching Supersonic Jet", *Journal of Flow Visualization*, **3** (2), pp 135-143
2. Chou, W.H., Hsiang, L.P., and Faeth, G.M., 1997, "Temporal properties of drop breakup in the shear breakup regime", **23**, *Int. J. Multiphase Flow*, pp 651-669.
3. Hsiang, L.P., and Faeth, G.M., 1995, "Drop deformation and breakup due to shock wave and steady disturbances", **21**, *Int. J. Multiphase Flow*, pp 545-560.
4. Knudsen, V.O., Wilson, J.V., and Anderson, N.S, 1948, "The attenuation of sound in fog and smoke" *J. Acoust. Soc. Amer.*, **20**, pp 849-857.
5. Kulick, J.D., Fessler, J.R., and Eaton, J.K., 1994, "Particle response and turbulence modification in fully developed channel flow", **277**, *J. Fluid Mechanics*, pp 109-134.
6. Krothapalli, A., Venkatakrishnan, L., Elavarasan, R, and Lourenco, L., "Supersonic jet noise suppression by water injection, AIAA Paper 2000-2025, June 2000.
7. Liang, P.Y., Eastes, T.W. and Gharakhari, A., 1988, "Computer simulations of drop deformation and drop breakup". *AIAA Paper No. 88-3142*,.
8. Marble, F.E., and Wooten, D.C., "Sound attenuation in a condensing vapor", 1970, *The Physics of Fluids*, **13**, pp 2657-2664.
9. Marble, F.E., and Candel, S.M., 1975 "Acoustic attenuation in fans and ducts by vaporization of liquid droplets", *AIAA Journal*, **13**, , pp 634-639.
10. Phillips, O.M., 1960, "On the generation of sound by supersonic turbulent shear layers", *J. Fluid Mech.*, **9**, pp. 1-28.
11. Samimy, M., and Lele, S.K., 1991, "Motion of particles with inertia in a compressible free shear layer, **3** (8), *Phys. Fluids A*, pp 1915-1923.